Proceedings of the ASME 28th International Conference on Ocean, Offshore and Arctic Engineering
OMAE 2009
May 31-June 5, 2009, Honolulu, Hawaii, USA

OMAE2009-80115

DYNAMIC INTERACTIONS BETWEEN THE VADOSE AND PHREATIC ZONES DURING BREAKING SOLITARY WAVE RUNUP AND DRAWDOWN OVER A FINE SAND BEACH

Heng Xiao
Department of Civil and Environmental Engineering
Princeton University
Princeton, NJ 08544
Email: xiao@princeton.edu

Yin L. Young
Department of Civil and Environmental Engineering
Princeton University
Princeton, NJ 08544
Email: yyoung@princeton.edu

Jean H. Prévost
Department of Civil and Environmental Engineering
Princeton University
Princeton, NJ 08544
Email: prevost@princeton.edu

ABSTRACT

The objective of this work is to investigate the dynamic interactions between the vadose and the phreatic zones during breaking solitary wave runup and drawdown over a fine sand beach. Extreme wave runup and drawdown in the nearshore region can lead to soil failure in the form of severe erosion, liquefaction, or slope instability. However, the physics of the nearshore region is difficult to simulate numerically due to the greatly varying time scales between the four governing processes: loading and unloading caused by wave runup and drawdown, propagation of the saturation front, pore pressure diffusion, and soil consolidation. Such processes are also difficult to simulate experimentally via model-scale wave tank studies due to the inability to satisfy all the similarity requirements for both the wave and the porous media in a 1g environment. Hence, the goal of this work is to perform a 1D study using a multiphase model to describe the transient responses of the species saturation, pore fluid pressure, effective stresses, and skeleton deformation. Results are shown for three simulations: (1) full-scale simulation, (2) 1:20 laboratory-scale simulation without scaling of the porous media, and (3) 1:20 laboratory-scale with consistent scaling of the soil permeability. The results suggest that the scaling of porous media between the pore fluids and soil skeleton has a significant influence on the transient response of both the vadose and the phreatic zones.

1 Introduction

Wave-induced bed responses in the near-shore region, particularly the region above the subsurface still water table, are of great interests to civil engineers, coastal engineers, geomorphologiests, and others. These responses including groundwater flow, bed displacement and stress, and pore water pressure have influences on various processes such as sediment transport, as well as chemical and biological transfer in the near-shore region. Fundamental understanding of these processes are also of vital importance to the safety of coastal slopes and coastal infrastructures.

Coastal engineers and geomorphologiests have long been interested in this region. Horn [1] reviewed the research activities toward improving the understanding of beach water-table and swash interactions, as well as their effects on sediment transport and beach accretion / erosion. Turner and Masselink [2] studied the influence of infiltration and exfiltration on cross-shore sediment transport via field observations and numerical simulations. Nielsen and Perrochet [3] experimentally studied the effects of capillary pressure on water-table dynamics. Li and Barry [4] studied the groundwater responses under wave motions with a coupled numerical model. The waves are modeled with nonlinear shallow water equations, the solution of which provides boundary conditions to the by the Laplace equation describing the groundwater flow. The only field variables present in this model are water height and velocity for waves and hydraulic head

for the groundwater flow, while the bed displacement and pore pressure fields are not modeled, which is a typical methodology utilized by coastal engineers.

On the other hand, civil engineers are interested in the static and dynamic responses of the soil under various loadings. The displacement and stress of the soil are of primary interests since soil (or rock) serves as the foundations and supports for most of the buildings, bridges, and other infrastructures. The interactions from the structures, the soil skeleton, and the pore fluids (water and/or air) are very complex and the different physical processes in the interactions are coupled and highly nonlinear. In the past few decades, much effort has been made toward advancing the fundamental understanding of the interactions between surface and subsurface flows. Biot [5] laid the foundation for the mechanics and dynamics of fluid-saturated porous media by extending the classical elasticity theories. Prévost [6, 7] was among the first to formulate the soil dynamics problem in the framework of porous media and analyzed the nonlinear transient soil responses by solving the equations with finite element methods. Similar efforts towards improving the understanding of the phenomena were made by Zienkiewicz and coworkers [8, 9]. In these models, the soil are assumed to be fully saturated with fluid. Field variables include pore fluid pressure and soil skeleton displacement. Meiri and Karadi [10] developed a finite element model to describe the two-phase flow of gas and liquid. With this numerical model, a gas percolation problem in the context of oil production was solved. The model was one-dimensional, with the interactions between the fluids (i.e. capillary pressure and relative permeability) and the compressibility of the fluids considered. However, the deformation of the soil skeleton was ignored, and the porosity was thus constant. The solubility of air and the volatility of water were neglected as well. Summarizing previous efforts, Zienkiewicz et. al. [11] developed a finite element model to solve fully saturated soil problems. Zienkiewicz et. al. [12] extended the formulation for unsaturated problems by modifying a "combined fluid/solid compressibility" term. The unsaturated formulation was used to simulate the collapse of the San Fernando earth dam in 1971. Other notable works considering the coupling of unsaturated flow and geomechanics include those by Rahman and Lewis [13] and Schrefler and Scotta [14], among others.

The difficulties underlying the modeling of unsaturated flow problem in deformable porous media are mainly associated with the non-linearity introduced by the relative permeability and the capillary pressure, and the complex interactions among the processes with a wide range of times scales. Although many researchers have developed numerical models to simulate the unsaturated flow problems, the fundamental physics of the problem is still not fully understood.

2 Objective

The objective of this work is to investigate the dynamic interactions between the vadose and the phreatic zones during breaking solitary wave runup and drawdown over a fine sand beach. More specifically, the goal is to advance the understanding of the consequence of improper scaling of the porous media during typical $1g$ wave tank studies of wave-soil interactions.

3 Mathematical Formulation

The problem of bed response under wave loading is formulated in the framework of porous media theory, where the constituents (sand grains, water, and air) are assumed to be individual continua, all interpenetrating each other and occupying the whole domain, each being regarded as a phase. If the inter-grain pores are almost completely occupied by one fluid, and other fluids do not play significant roles, the medium can be modeled as a saturated porous medium. In this case, problem is formulated in terms of soil skeleton displacements ($\mathbf{u}$) and pore pressures (p). Otherwise, if two or more fluids jointly occupy the inter-grain pores, the mobility of the pore fluids may interfere with each other and capillary pressure may be important. In such cases, the medium needs to be modeled as an unsaturated porous media, i.e., in addition to skeleton displacements and pore pressures, the saturation for each of the species (S_i) needs to be described. The two formulations are presented as follows.

3.1 Saturated Soil

The soil skeleton and the pore water in the sediment bed are modeled in the framework of poromechanics theory [15]. The soil deposit is assumed to be fully saturated (with either water or air). The following equations are solved:

$$\nabla \cdot \underline{\sigma} + [(1-\phi)\rho_s + \phi\rho_f]\,\mathbf{b} = 0 \tag{1}$$

$$\phi \frac{d\rho_f}{dt} + \nabla \cdot \mathbf{q} + \rho_f \frac{d\phi}{dt} = 0 \tag{2}$$

with

$$\frac{d\phi}{dt} = b\nabla \cdot \mathbf{v}^s + \frac{1}{N}\frac{dp_f}{dt} \tag{3}$$

and mass flux of the pore fluid

$$\mathbf{q} = \rho_f \bar{\mathbf{q}}^f \tag{4}$$

where fluid volume flux $\bar{\mathbf{q}}^f$ is modeled according to Darcy's law:

$$\bar{\mathbf{q}}^f = -\frac{\mathbf{k}}{\mu_f} \cdot [\nabla p_f - \rho_f \mathbf{b}] \tag{5}$$

The quantities b and N are defined as [15]:

$$\frac{1}{N} = \frac{b-\phi_0}{K_s} \qquad (6)$$
$$b = 1 - \frac{K}{K_s}$$

where $\underline{\sigma}$ = total stress tensor of the mixture; ϕ = Lagrangian porosity of the soil; ϕ_0 = initial porosity; ρ_s and ρ_f: solid and fluid density; $\mathbf{b}$ = body force (gravity in this study); p_f = pore fluid pressure; $\mathbf{v}^s$ = solid velocity; $\mathbf{k}$ = intrinsic permeability tensor of the soil skeleton (for isotropy it is replaced with a scalar k); μ_f = dynamics viscosity of the pore fluid; b = Biot's coefficient; K and K_s: bulk moduli of the solid matrix and the grains, respectively.

For porous media with saturated fluid (the pores are completely occupied by one fluid), the change of fluid density is related to the change of pore pressure:

$$\frac{d\rho_f}{\rho_f} = C_f dp_f \qquad (7)$$

where C_f is the compressibility of the pore fluid.

The solid stresses and velocities are expressed in terms of solid displacement field $\mathbf{u}^s$ as follows:

$$\underline{\sigma} = \underline{\sigma}^s - bp_f\underline{\delta} \qquad (8)$$
$$\underline{\sigma}^s = \mathbf{C} : \underline{\varepsilon}^s \qquad (9)$$
$$\underline{\varepsilon}^s = \nabla_{()}\mathbf{u}^s \qquad (10)$$
$$\mathbf{v}^s = \frac{\partial \mathbf{u}^s}{\partial t} \qquad (11)$$

where $\mathbf{C}$ is the constitutive tensor (fourth-order); The symbol ":" denotes the contraction product of two tensors; $\underline{\varepsilon}^s$ = strain of the skeleton; $\nabla_{()}\mathbf{u}^s = (\nabla\mathbf{u}^s + \mathbf{u}^s\nabla)/2$ is the symmetric part of tensor $\nabla\mathbf{u}^s$; $\underline{\delta}$ is second order unit tensor; p_0 is initial fluid pressure; Equation (8) shows that the total stress of the mixture ($\underline{\sigma}$) is decomposed into effective stress acting on the soil skeleton ($\underline{\sigma}^s$) and pressure carried by the pore fluid (p_f).

3.2 Unsaturated Soil

With the presence of n_p fluid phases, extra (n_p-1) saturation equations need to be solved in addition to the linear momentum balance in Equation (1) and the total mass balance in Equation (2). With the presence of several fluids in the pores, the apparent fluid density is written as

$$\rho_f = \sum_{\alpha=1}^{n_p} \rho_\alpha S_\alpha \qquad (12)$$

where n_p is the number of fluid phases; the subscript α is the fluid phase index, which could be either l (liquid/water) or g (gas/air) in this study. The momentum balance is the same as in Equation (1). The fluid mass balance takes the same form as in Equation (2). The first term is now written as follows to accommodate the presence of several fluids:

$$\frac{d\rho_f}{dt} = \frac{d}{dt}\left[\sum_{\alpha=1}^{n_p}\rho_\alpha S_\alpha\right] = \left[\sum_{\alpha=1}^{n_p}\rho_\alpha S_\alpha C_\alpha\right]\frac{dP}{dt}, \qquad (13)$$

which is an approximation. P is the global pressure. In the second term of Equation (2), the *total mass flux* $\mathbf{q}$ is now defined as

$$\mathbf{q} = \sum_{\alpha=1}^{n_p}\rho_\alpha\bar{\mathbf{q}}_\alpha = -\left(\sum_{\alpha=1}^{n_p}\rho_\alpha k_\alpha\right)\mathbf{k}\cdot[\nabla P - \bar{\rho}\mathbf{b}] \qquad (14)$$

where $\bar{\mathbf{q}}_\alpha$ is the volume flux of phase α; $\bar{\rho}$ is defined as

$$\bar{\rho} = \frac{\sum_{\alpha=1}^{n_p}\rho_\alpha^2 k_\alpha}{\sum_{\alpha=1}^{n_p}\rho_\alpha k_\alpha} \qquad (15)$$

and

$$k_\alpha = \frac{k_{r\alpha}}{\mu_\alpha} \qquad (16)$$

is the mobility of phase α, where $k_{r\alpha}$ is the relative permeability of phase α. The saturation S_α of phase α is obtained from the saturation equation:

$$\phi\frac{d(\rho_\alpha S_\alpha)}{dt} + \nabla\cdot(\rho_\alpha\bar{\mathbf{q}}_\alpha) + \rho_\alpha S_\alpha\frac{d\phi}{dt} = 0 \qquad (17)$$

where the phase max fluxes are expressed as follows:

$$\rho_\alpha\bar{\mathbf{q}}_\alpha = \frac{\rho_\alpha k_\alpha}{\sum_{\beta=1}^{n_p}\rho_\beta k_\beta}\mathbf{q} \qquad (18)$$
$$+ \sum_{\beta=1}^{n_p}\rho_\beta k_\beta\mathbf{k}\cdot\left[\frac{\rho_\alpha k_\alpha}{\sum_{\beta=1,\beta\neq\alpha}^{n_p}\rho_\beta k_\beta}\left[\nabla P_c^{\alpha\beta} + (\rho_\alpha - \rho_\beta)\mathbf{b}\right]\right]$$

where $P_c^{\alpha\beta}$ is the capillary pressure between phase α and β. Only (n_p-1) saturation equations need to be solved because of the constraint $\sum_{\alpha=1}^{n_p} S_\alpha = 1$.

In the equations above, capillary pressure between the phases is ignored, i.e. $P_c^{\alpha\beta} = 0$, and the effect of capillary pressure will be investigated in future studies. As a consequence, the pressure for different phases p_α are all equal to the global pressure P. The pressure is denoted as p_f hereafter, or p when no confusion is caused. The relative permeability need modeling to close the system. In practice, it is formulated as empirical functions of the saturation S_α. The Corey's curve is adopted for the relative permeability (Corey, 1954):

$$k_{rl} = \hat{S}^4 \tag{19}$$

$$k_{rg} = (1-\hat{S})^2(1-\hat{S}^2) \tag{20}$$

$$\text{with} \quad \hat{S} = \frac{S_l - S_{lr}}{1 - S_{lr} - S_{gr}} \tag{21}$$

where S_{lr} = residual saturation for the liquid (water); S_{gr} = residual saturation for the gas (air); $\hat{S}$ = normalized saturation; The residual saturation is the threshold saturation for a phase below which this phase is not mobile.

4 Numerical Methods

The fully coupled equations of displacements (**u**) and pressure (p) are solved simultaneously with a stabilized Galerkin finite element method. The saturation equations are solved using vertex-centered finite volume method with an upwinding scheme [16] and are coupled to pressures and displacements with a staggered approach with iterations. Other details of the algorithms are discussed in Refs. [17, 18]. A finite element / finite volume analysis program `DynaFlow` is used for the simulations [19].

5 Problem Definition

When wave-soil interaction problems are studied in laboratories, it is often difficult to scale the sand particle diameters since the change of particle diameter may lead to changes of other properties such as cohesion, particle weight, and particle settling velocity. As a result, soil experiments often have to be conducted with improperly scaled sand (soil). It is important to assess the effect of improper scaling of the bed material on the transient responses.

In this section, simulations are conducted to compare the response of a full-scale model to a laboratory-scale model with a geometric length scale ratio of 1 : 20. The model-scale wave simulations are assumed to satisfy Froude number similarity, and thus the ratio of time scales between the model and the prototype is $1 : \sqrt{20}$. Three scenarios are examined: (1) the full-scale model; (2) 1:20 laboratory-scale model with the same soil as in the prototype; and (3) 1:20 laboratory-scale model with the soil permeability is scaled according to $k_{\text{prototype}}/k_{\text{model}} = 20^{3/2}$, in order to correctly scale pressure diffusion and consolidation time scales. The laboratory-scale simulations are referred to as cases (2) and (3), respectively Details of the scaling issues are presented in Ref. [20].

In both laboratory-scale case studies, it is assumed that the porosity and the Young's modulus of the soil, and the compressibility and viscosity of the fluids are the same between the all laboratory-scale models and the prototype.

In all the simulations that follows, the initial saturation is $S_0 = 95\%$ in the region below the initial water table (phreatic zone) and zero above the water table (vadose zone). The initial pressure is atmospheric (10^5 Pa) at the top surface and the pressure distribution is hydrostatic elsewhere in the simulation domain.

Body force (gravity) is considered in all the simulations. The displacements are initialized as follows: the domain is first allowed to consolidate under gravity with the presence of the hydrostatic pressure from the initial water column until the system reaches a steady state, and then the displacements of the whole soil domain are set to be zero. Therefore, the initial stresses and strains are in equilibrium state in the whole domain. This treatment ensures that any displacements obtained afterwards are due solely to wave actions, and so are the stress and strain variations.

The top boundary is subject to the surface water pressure depending on the loading type, while the effective stresses at the top boundary are kept zero. The pressures at the bottom boundary are fixed such that the initial hydrostatic pressures in the soil column are balanced exactly. The bottom boundary is fixed with no displacement. The saturation is 100% at the top surface whenever there is external pressure (other than atmospheric pressure) applied at the top. The saturation is fixed at 95% at the bottom surface. All simulations are conducted with 200 two-node elements of uniform size unless noted otherwise. Grid convergence studies are conducted and good convergence has been observed for all the cases.

To ensure the simulations are conducted in appropriate time domains and with suitable time steps, the time scales of the all the cases are first estimated as presented in Table 1. The results are presented in Table 3, based on which the simulation time duration and time step size are determined. The estimated times also facilitates interpretation of the results. Physical parameters used in the simulation are presented in Table 2. More details about the derivation of the characteristic time scales can be found in Ref. [20].

All the simulations shown below are conducted using the unsaturated formulation presented in Section 3.2. However, when the saturation propagation is negligible, the unsaturated formulation is equivalent to the saturated formulation in Section 3.1, which is easier for theoretical analysis.

Table 1. Expressions for the characteristic time scales in unsaturated flows. H = initial wave height; d = offshore still water depth; θ = bed slope; μ = dynamics viscosity; ϕ: porosity; L = soil column depth; k = permeability C_m = compressibility of the soil matrix. Refer to Figure 1. The bottom is the origin of x axis.

Physical process	Time scale
Wave propagation	$T_{cw} = \frac{3H^{0.3}d^{0.2}}{\tan\theta\sqrt{g}}$
Saturation front propagation	$T_{cs} = \frac{\phi}{4}\frac{\mu}{k}\frac{L}{dp/dx}$
Pressure diffusion pore fluid	$T_{cp} = \frac{L^2\phi\mu C_f}{k}$
Consolidation	$T_{cc} = \frac{L^2\mu C_m}{k}$

Table 2. Common physical parameters used in all the simulations (unless noted otherwise).

Parameter	Quantity and unit
Gravity constant (g)	10 m/sec^2
Young's modulus of skeleton (E)	1.5×10^8 Pa
Poisson's ratio of skeleton (ν)	0.2
Density of sediment/soil grains (ρ_s)	2650 kg/m^3
Intrinsic permeability of skeleton (k)	1.5×10^{-11} m^2
Porosity of sediment/soil (ϕ)	0.4
Compressibility of pure water (C_w)	4.6×10^{-10} m^2/N
Compressibility of air (C_a)	1.0×10^{-5} m^2/N
Density of water (ρ_w)	1.0×10^3 kg/m^3
Density of air (ρ_a)	1.0 kg/m^3
Dynamics viscosity of water (μ_w)	1.0×10^{-3} kg$\cdot$m/sec
Dynamics viscosity of air (μ_a)	1.8×10^{-5} kg$\cdot$m/sec
Residual saturation of liquid/water (S_{lr})	3%
Residual saturation of gas/air (S_{gr})	3%

6 Results

6.1 Full-Scale Simulation

Consider a soil column on the shore-face of a beach with a constant slope (1:15) as shown in Figure 1. For the full-scale problem, the soil column is located 30 m onshore. The depth of the soil column is 20 m with a vadose zone of 2 m. The beach is subject to a solitary waves of with an initial height of 12 m at a still water depth of d=20 m, which would break before arriving at the shoreline and then climb up onshore in the form of a bore. The propagation of the wave is modeled with a hybrid numerical model which solves the nonlinear shallow water equations for the post-breaking region and the Boussinesq equations for the pre-breaking region [21]. The time series of water depth at the location of the soil column is obtained from numerical simulations with the hybrid model. The load applied on the top of the soil column is assumed to be the hydrostatic pressure from the water column. The simulation results for the full-scale model is presented in Figure 2 (a), with the pressure and time normalized as explained in the figure caption.

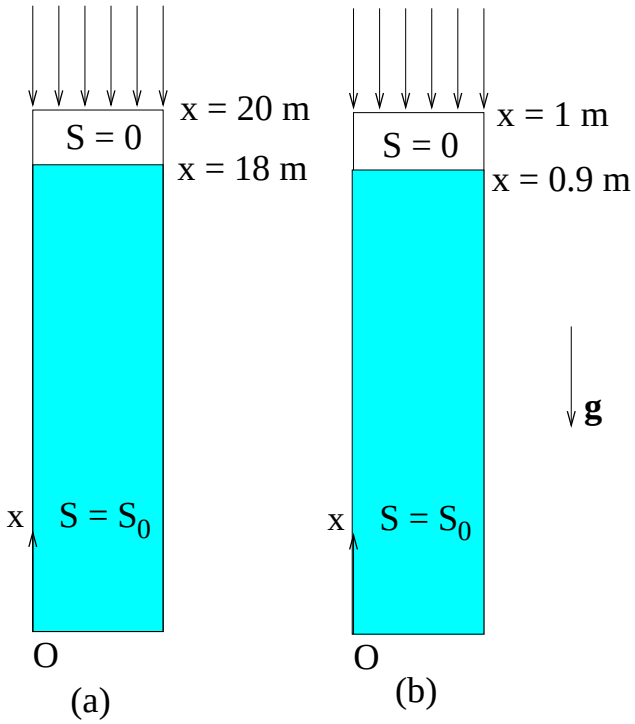

Figure 1. Schematic setup of the simulations. (a) full-scale model, case (1); (b) laboratory-scale model, cases (2), and (3).

6.1.1 1:20 Model-Scale Simulation without Scaling the Soil

The result for the laboratory-scale model simulations without properly scaling the soil permeability (case (2)) is presented in Figure 2 (b). Comparing the model-scale pore pressure response shown in Figure 2(b) with the full-scale pore pressure response shown in plot (a), it can be seen that the simulation without scaling the soil permeability in case (2) gives qualitatively incorrect predictions, i.e. the pressure decay along the depth is much larger and faster than the prototype simulation. The fundamental differences between the results are the mecha-

nisms causing the pressure variation. In the prototype (plot (a)), the pressure variations at the bottom two locations ($x = 0.5L$ and $x = 0.875L$, or 10 m and 18.5 m, respectively) are dominated by the "squeezing effects" as a result of the pore space contraction, while that at the top location ($x = 0.975L$, or 19.75m) is dominated by pressure diffusion, which is confirmed by the slight delay of the pressure compared to the input pressure at the top ($x = L$). In the laboratory-scale model results without scaling the soil permeability in plot (b), the "squeezing" effects seem to dominate at all the locations. However, since the permeability is much larger than the properly scaled value, the drainage condition is better than that in the prototype, and thus the pressure increase caused by the loading is not as large as in the prototype.

6.1.2 1:20 Model-Scale Simulation with Porous Media Scaling Preserving Pressure Responses Further investigations are conducted to explore the possibility of achieving perfectly scaled pore pressure responses by choosing a permeability scaling ratio alone. As mentioned above, Froude number is preserved for the model-scale wave experiments, and the time is scaled according to:

$$t_{\text{prototype}}/t_{\text{model}} = \sqrt{\lambda} \tag{22}$$

where λ is the length scale ratio.

To obtain properly scaled pressure and effective responses, the time scale of the porous flow should also be scaled as in Equation (22). This is achieved by choosing $\Lambda[k] = \lambda^{3/2}$, according to the expressions for the time scales in Table 1. To verify the analysis above, a simulation is conducted for a laboratory-scale case with the permeability scaled according to the ratio $\lambda^{3/2}$, i.e. $k_{\text{model}} = 1.5 \times 10^{-11}/20^{3/2} = 1.67 \times 10^{-13}$ m^2. The result is presented in Figure 2(d). It can be seen that the pore pressure responses are scaled perfectly. The effective stress is also scaled perfectly, but is not shown here due to space limitations.

In summary, the analysis above demonstrated that using the same soil in the experiment as in the prototype does not give qualitatively correct results. Scaling soil permeability k according to $\lambda^{3/2}$ gives perfectly scaled transient pressure and stress responses, which also confirms that the mechanisms responsible for the transient responses in the porous media under external loading are pressure diffusion and consolidation.

It should be noted, however, the analysis shown above represent a simplified and idealized problem. In reality, it is difficult to change the soil permeability while keeping the porosity and Young's modulus constant. Furthermore, other responses such as saturation propagation rate and displacement are not scaled properly since other material properties are not scaled properly. In addition, the analysis above assumes that the experiment is conduced in a one-gravity acceleration ($1g$) environment. By conducting experiments in centrifuges, acceleration environments

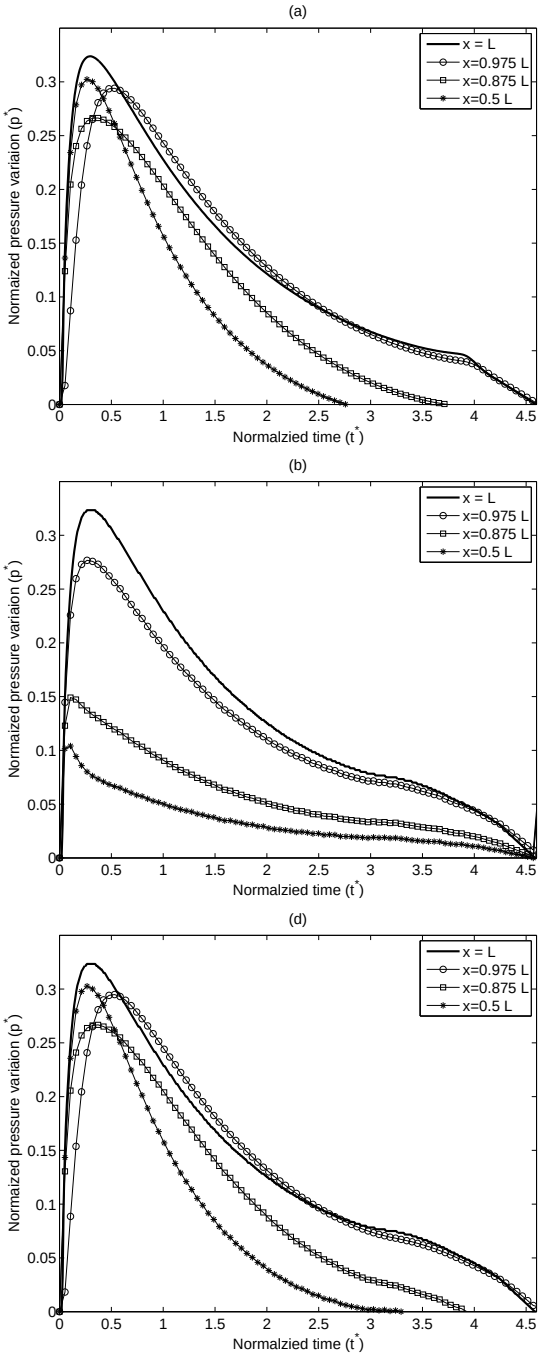

Figure 2. Time series of the normalized pore pressures at three locations along a soil column during the first solitary wave runup and drawdown. (a) Case (1): prototype with soil depth L = 20 m. (b) Case (2): laboratory-scale model with the same soil as in prototype; (c) Case (3): laboratory-scale model with properly scaled soil permeability $k = 1.67 \times 10^{-13}$ m^2. L = 1 m for the laboratory-scale models (b) and (c). The pressure is normalized as $p^* = p/\rho_w gH$, where H is the offshore wave height. The time is normalized as $t^* = t\sqrt{g/d}$, where d is the initial offshore still water depth.

greater than $1g$, can be achieved and thus different scaling relationships are possible. However, conducting experiments on centrifuges significantly increases the operation costs and the complexity of the experiments. Furthermore, the scales of the experiments that can be conducted on centrifuges are seriously limited compared to those in conventional wave flumes.

7 Conclusion

Unsaturated flow in porous media is a multi-physics problem with greatly varying time scales. It is essential to choose proper time scales corresponding to the physical phenomena that needs to be capture in order to correctly model the phenomena. Simulations suggest that it is essential to correctly scale the permeability of the soil in the experiments where the soil responses are studied. Improper scaling of the soil permeability may lead to qualitatively incorrect experimental results, which should not be extrapolated to prototypes. Via time scale analysis, a permeability scaling relation to achieve perfectly scaled transient pore pressure responses is proposed, which may be valuable for future large-scale experiments studying wave-soil interactions.

REFERENCES

[1] Horn, D. P., 2002. "Beach groundwater dynamics". *Geomorphology,* **48**, pp. 121–146.

[2] Turner, I. L., and Masselink, G., 1998. "Swash infiltration-exfiltration and sediment transport". *J. Geophy. Res.,* **103**(C13), pp. 30813–30824.

[3] Nielsen, P., and Perrochet, P., 2000. "Watertable dynamics under capillary fringes: experiments and modelling". *Advances in Water Resources,* **23**, pp. 503–515.

[4] Li, L., and Barry, D. A., 2000. "Wave-induced beach groundwater flow". *Advances in Water Resources,* **23**, pp. 325–337.

[5] Biot, M., 1941. "General theory of three-dimensional consolidation". *J. Appl. Phys.,* **12**(2), pp. 155–164.

[6] Prévost, J. H., 1980. "Mechanics of continuous porous media". *Int. J. Eng. Sci.,* **18**(5), pp. 787–800.

[7] Prévost, J. H., 1982. "Nonlinear transient phenomena in saturated porous media". *Computer Methods in Applied Mechanics and Engineering,* **30**(1), pp. 3–18.

[8] Zienkiewicz, O. C., 1982. "Basic formulation of static and dynamic behaviour of soil and other porous material". In *Numerical methods in geomechanics*, J. Martins, ed. Boston and London: D. Reidel.

[9] Zienkiewicz, O., and Shiomi, T., 1984. "Dynamic behaviour of saturated porous media; the generalized Biot formulation and its numerical solution". *Int. J. Num. Ana. Meth. Geomech.,* **8**, pp. 71–96.

[10] Meiri, D., and Karadi, G. M., 1982. "Simulation of air storage aquifer by finite element model". *Int. J. Num. Ana. Meth. Geomech.,* **6**, pp. 339–351.

[11] Zienkiewicz, O., Chan, A., M.Pastor, Paul, D., and Shiomi, T., 1990. "Static and dynamic behaviour of soils: a rational approach to quantitative soutions. I. fully saturated problems". *Proc. R. Soc. London,* **A**(429), pp. 285–309.

[12] Zienkiewicz, O., Xie, Y., Schrefler, B., Ledesma, A., and Bi$\hat{c}$ani$\hat{c}$, N., 1990. "Static and dynamic behaviour of soils: a rational approach to quantitative soutions. I. fully saturated problems". *Proc. R. Soc. London,* **A**(429), pp. 285–309.

[13] Rahmann, N. A., and Lewis, R. W., 1999. "Finite element modelling of multiphase immiscible flow in deforming porous media for subsurface systems". *Compters and Geotechnics,* **24**, pp. 41–63.

[14] Schrefler, B., and Scotta, R., 2001. "A fully coupled dynamic model for two-phase fluid flow in deformable porous media". *Computer Methods in Applied Mechanics and Engineering,* **190**, pp. 3223–3246.

[15] Coussy, O., 2004. *Poromecahnics*. John & Wiley, Hoboken, NJ.

[16] LeVeque, R. J., 2002. *Finite Volume Methods for Hyperbolic Problems*. Cambridge University Press.

[17] Prévost, J. H., 1983. "Implicit-explicit schemes for nonlinear consolidation". *Computer Methods in Applied Mechanics and Engineering,* **39**, pp. 225–239.

[18] Prévost, J. H., 1997. "Partitioned solution procedure for simultaneous integration of coupled-field problems". *Communications in numerical methods in engineering,* **13**, pp. 239–247.

[19] Prévost, J. H., 1983. *DynaFlow: A nonlinear transient finite element analysis programme*. Dept. of Civil Engineering, Princeton University, Princeton, NJ. (Last updated 2008).

[20] Xiao, H., Young, Y., and Prévost, J. Time scales and scaling analysis of soil responses during wave runup and drawdown. Under Preparation.

[21] Xiao, H., Young, Y. L., and Prévost, J. H., 2009. "Runup and drawdown of breaking solitary waves over a fine sand beach. part ii: Numerical simulation". *Marine Geology*. Under review.

ACKNOWLEDGMENT

The authors would like to acknowledge funding by the National Science Foundation through the NSF George E. Brown, Jr. Network for Earthquake Engineering Simulation (grant no. 0530759) and through the NSF CMMI grant no. 0653772.

Table 3. Setup and approximate characteristic time scales of the cases simulated in this study, estimated based on the formulas in Table 1 and the physical parameters in Table 2.

Case number and description	(1) Prototype	(2) Lab scale	(3) Lab scale	Unit
Permeability	1.5×10^{-11}	1.5×10^{-11}	1.67×10^{-13}	m^2
Offshore wave height	12	0.6	0.6	m
Soil column height	20	1	1	m
Vadose zone height	2	0.1	0.1	m
Wave loading	55	10	10	sec
Water penetration	4500	230	20000	sec
Water pressure diffusion	10	0.03	2.4	sec
Air pressure diffusion	2000	5	430	sec
Consolidation	160	0.5	36	sec